

# IS HIGH VARIANCE UNAVOIDABLE IN RL? A CASE STUDY IN CONTINUOUS CONTROL

Johan Bjorck, Carla P. Gomes, Kilian Q. Weinberger  
Cornell University

## ABSTRACT

Reinforcement learning (RL) experiments have notoriously high variance, and minor details can have disproportionately large effects on measured outcomes. This is problematic for creating reproducible research and also serves as an obstacle for real-world applications, where safety and predictability are paramount. In this paper, we investigate causes for this perceived instability. To allow for an in-depth analysis, we focus on a specifically popular setup with high variance – continuous control from pixels with an actor-critic agent. In this setting, we demonstrate that variance mostly arises early in training as a result of poor “outlier” runs, but that weight initialization and initial exploration are not to blame. We show that one cause for early variance is numerical instability which leads to saturating nonlinearities. We investigate several fixes to this issue and find that one particular method is surprisingly effective and simple – normalizing penultimate features. Addressing the learning instability allows for larger learning rates, and significantly decreases the variance of outcomes. This demonstrates that the perceived variance in RL is not necessarily inherent to the problem definition and may be addressed through simple architectural modifications.

## 1 INTRODUCTION

With the advent of deep learning, reinforcement learning (RL) with function approximators has become a promising strategy for learning complex behavior (Silver et al., 2017; Mnih et al., 2015). While RL can work remarkably well, deep RL experiments have been observed to exhibit high variance (Chan et al., 2019; Clary et al., 2019; Lynnerup et al., 2020). Specifically, the rewards obtained by RL agents commonly vary significantly depending on the random seeds used for training, even if no other modifications are made. Implementation level details often have an outsized effect on performance (Engstrom et al., 2020) and even hardware scheduling can significantly affect outcomes (Henderson et al., 2017). In comparison to RL, computer vision and natural language processing (NLP) experiments often have lower variance (Bouthillier et al., 2021).

High variance is problematic for creating reproducible RL research, and achieving statistically significant results over large RL benchmarks is often prohibitively time-consuming (Colas et al., 2018; Agarwal et al., 2021). Furthermore, this variance provides an obstacle for real-world applications of RL, where safety and predictability can be critical (Garcia & Fernández, 2015; Srinivasan et al., 2020). Relevant applications where RL is already being evaluated include medical testing (Bastani et al., 2021), autonomous vehicles (Bellemare et al., 2020) and communications infrastructure (Liu et al., 2020). RL agents are typically evaluated on the average performance, but for these sensitive real-world applications, the drastic performance drop for the worst-performing training runs could yield disastrous outcomes.

In this paper, we aim to investigate causes for high variance in RL. To limit the paper’s scope and computational footprint we focus on continuous control from pixels with a SOTA actor-critic algorithm (Lillicrap et al., 2015; Yarats et al., 2021b). This is a popular setup that exhibits high variance, and where actor-critic algorithms often give SOTA results (Laskin et al., 2020b;a; Kostrikov et al., 2020). Additionally, this class of tasks is relatively close to real-world robotics (Zhan et al., 2020).

In this setting, we first show that variance often is dominated by outlier runs that fail early in the learning process and never recover. It is natural to hypothesize that the typical sources of randomness, network initialization and initial exploration, are to blame. However, we demonstrate that

these do in fact have little impact on the final performance. We similarly provide experiments that suggest that neither poor feature representations nor excessive sensitivity of the environment are at fault. We instead demonstrate that numerical instability can drive most of the variance and show that exploding activations that saturate action distributions can often yield poor performance. We propose a few methods to avoid these issues and find that they do indeed decrease variance and improve average performance. The most effective method is simply normalizing the penultimate features which avoids exploding activations by design. We further show that our proposed approaches reliably enable larger learning rates and decrease variance significantly across tasks. In fact, by combining multiple approaches we can reduce the variance by close to two orders of magnitude on a humanoid locomotion task. We conclude that simply addressing numerical stability in the network parametrization is a promising avenue for stabilizing RL agents. Our experiments also suggest that high variance is not necessarily inherent to the RL setting. We summarize our contributions:

- We provide extensive experiments on the variance of a popular continuous control setup. We show that outliers often dominate the variance, but that poor initialization, sensitive environments, and feature learning are likely not the issues.
- We show that saturating action distributions and exploding activations can cause outlier runs and propose several methods to avoid such cases.
- We demonstrate that the proposed methods significantly decreases variance while improving average performance. This shows that addressing stability in the network parametrization is a promising avenue for stabilizing RL agents.

## 2 BACKGROUND

**Reinforcement Learning.** Reinforcement learning tasks can be formulated as Markov decision processes (MDPs) defined by a state-space  $\mathcal{S}$ , an action space  $\mathcal{A}$ , transition probabilities  $P$ , and a reward distribution  $r$  (Sutton & Barto, 2018). For continuous control tasks, the action space  $\mathcal{A}$  and the state space  $\mathcal{S}$  are typically continuous. Each dimension of the action space  $\mathcal{A}$  might for example correspond to a joint of a robotic arm, and the space is often bounded to account for physical limitations, e.g., how much force the robotic arm can exert. A common setting is simply  $\mathcal{A} = [-1, 1]^{dim(\mathcal{A})}$ . At every time step  $t$ , the agent is in some state  $\mathbf{s}_t \in \mathcal{S}$  and takes an action  $\mathbf{a}_t \in \mathcal{A}$  to arrive at a new state  $\mathbf{s}_{t+1} \in \mathcal{S}$ . The transition between states given an action is random with transition probability  $P : \mathcal{S} \times \mathcal{S} \times \mathcal{A} \rightarrow [0, \infty)$ . Given some action  $\mathbf{a}_t$  at timestep  $t$ , the agent also receives a reward  $r_t$  from the reward distribution  $r$ . When benchmarking RL agents, it is common to measure performance by the cumulative rewards  $\sum_t r_t$ .

**DDPG.** Deep Deterministic Policy Gradients (DDPG) (Lillicrap et al., 2015) is an algorithm for continuous control with roots in Q-learning (Watkins, 1989). Together with its offshoot soft actor-critic (SAC) (Haarnoja et al., 2018), DDPG forms the backbone of many state-of-the-art algorithms for continuous control (Laskin et al., 2020b;a; Kostrikov et al., 2020; Yarats et al., 2021b). DDPG uses a neural network (the *critic*) to predict the Q-value  $Q_\phi(\mathbf{a}_t, \mathbf{s}_t)$  for each state-action pair. The parameters  $\phi$  of the critic are trained by minimizing the soft Bellman residual:

$$\mathbb{E} \left( Q_\phi(\mathbf{a}_t, \mathbf{s}_t) - [r_t + \gamma \mathbb{E}[\hat{Q}(\mathbf{a}_{t+1}, \mathbf{s}_{t+1})]] \right)^2. \quad (1)$$

Here,  $r_t$  is the reward obtained and  $\mathbb{E}[\hat{Q}(\mathbf{a}_{t+1}, \mathbf{s}_{t+1})]$  is the Q-value estimated by the *target* critic – a network whose weights can e.g. be the exponentially averaged weights of the critic. One can also use multi-step returns for defining the critic loss function (Sutton, 1988). The policy  $\pi(\mathbf{s}) = \arg \max_{\mathbf{a}} Q_\phi(\mathbf{s}, \mathbf{a})$  is intractable since it requires finding  $\arg \max$  over a continuous action space. Instead the policy is given by an *actor*-network (with parameters  $\theta$ ), which maps each state  $\mathbf{s}_t$  to a distribution  $\pi_\theta(\mathbf{s}_t)$  over actions. The action is obtained by first sampling from a diagonal normal distribution where the mean  $\boldsymbol{\mu}_\theta(\mathbf{s})$  is given by the actor-network and the standard deviation  $\sigma_t$  might depend on time  $t$ . Thereafter a tanh non-linearity is applied elementwise to ensure  $\mathbf{a} \in [-1, 1]^n$  for  $n = dim(\mathcal{A})$ . This procedure defines the policy distribution, formally we have

$$\mathbf{a}_\theta^{pre}(\mathbf{s}) = \boldsymbol{\mu}_\theta(\mathbf{s}) + \sigma_t \times \boldsymbol{\epsilon}, \quad \boldsymbol{\epsilon} \sim \mathcal{N}(0, 1) \quad (2)$$

$$\mathbf{a}_\theta(\mathbf{s}) = \tanh(\mathbf{a}_\theta^{pre}(\mathbf{s})) \quad (3)$$

By sampling  $\epsilon$  we obtain an action  $\mathbf{a}_\theta$  from the policy  $\pi_\theta(\mathbf{s})$ . Since the Q-values correspond to the expected discounted rewards, the actions  $\mathbf{a}_\theta$  should maximize  $Q_\phi(\mathbf{a}_\theta, \mathbf{s})$ . Thus, to obtain a gradient update for the actor one uses the gradient  $\nabla_\theta Q_\phi(\mathbf{a}_\theta, \mathbf{s})$ , effectively calculating gradients *through* the critic network. In control from pixels, the state  $\mathbf{s}$  is typically an image processed by a small convolutional network. Image augmentations can dramatically improve performance in this setting (Kostrikov et al., 2020; Laskin et al., 2020a), and has become a standard method during training.

### 3 BENCHMARKING VARIANCE

#### 3.1 EXPERIMENTAL SETUP

There is a large number of available RL agents and environments to consider. To limit the papers the scope and computational footprint, we consider continuous control from pixels with an actor-critic algorithm. Continuous control from pixels is an environment type close to real-world applications such as autonomous driving (Kiran et al., 2021) and robotics (Zhu et al., 2020). Investigating causes of high variance in this domain could therefore have a large potential impact on downstream applications. We consider the standard continuous control benchmark deepmind control (dm-control) (Tassa et al., 2020). Within dm-control, a long line of state-of-the-art models relies on the actor-critic setup (Laskin et al., 2020b;a; Kostrikov et al., 2020; Yarats et al., 2021b). We consider DDPG (Lillicrap et al., 2015), using the recent data-augmentation based implementation of Yarats et al. (2021b) which provides state-of-the-art performance and runs fast. We use the default hyperparameters that Yarats et al. (2021b) uses on the *medium* benchmark (listed in Appendix A) throughout the paper. We will refer to this agent as the *baseline* agent. We are interested in using a large number of random seeds to obtain accurate statistics and thus need to limit the number of environments we consider. To select environments we simply rank the dm-control tasks based upon their relative variance as measured by Yarats et al. (2021a). We select the five tasks with the highest relative variance – finger turn hard, walker walk, hopper hop, acrobat swingup, and reacher hard (see Table 5 in Appendix A for details). We will refer to these as *environments* or *tasks* interchangeably. For each run, we train the agent for one million frames, or equivalently 1,000 episodes, and evaluate over ten episodes. We use 10 or 40 seeds for each method we consider, these are not shared between experiments, but we reuse the runs for the baseline agent across figures.

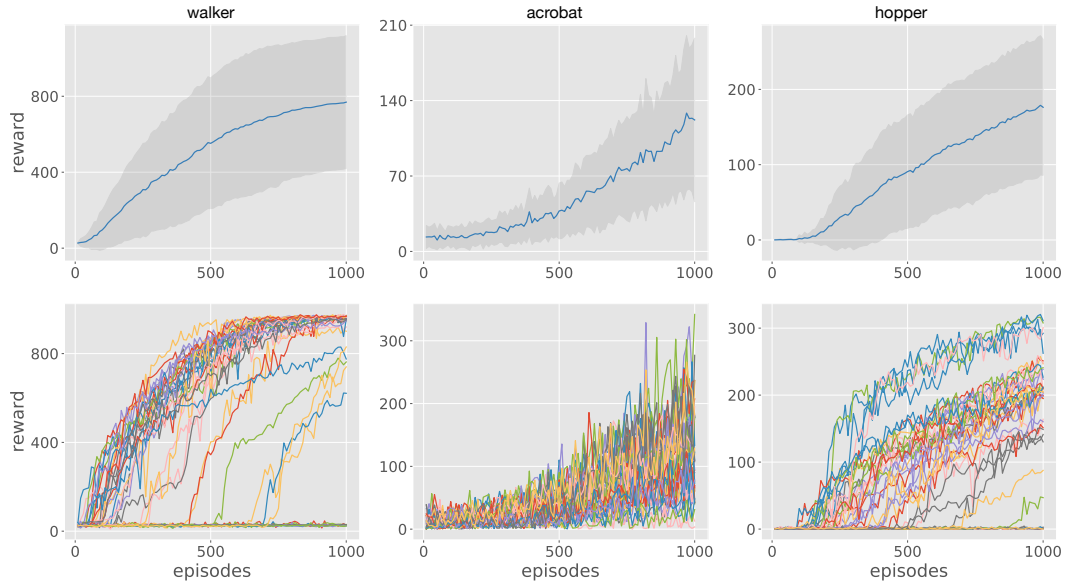


Figure 1: Learning curves over 40 seeds for the baseline agent. The upper row shows the mean reward with one standard deviation indicated by shading. The bottom row shows learning curves for individual runs. The high variance is often caused by a few outlier runs that completely fail to learn. This is especially clear in the walker task. Removing such outlier runs would decrease the variance.

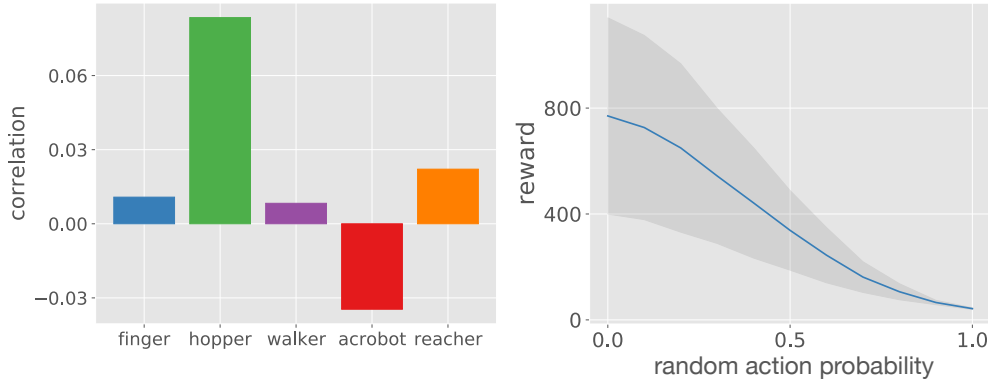


Figure 2: **(Left)** Correlation between runs that share network initialization and starting experience, but otherwise have independent other sources of randomness (e.g. from mini-batch sampling). Across all tasks, the correlation is small. This suggests that initialization and starting experience have limited effect on the outcomes. **(Right)** The average reward for the walker task when interpolating between a learned policy (random action probability = 0) and random policy (random action probability = 1). The rewards obtained decrease gracefully as we adopt a more random policy. This suggests that the environment is relatively forgiving with respect to actions.

### 3.2 VERIFYING VARIANCE

We first aim to verify that the environments indeed do exhibit high variance. To this end, we run the baseline algorithm with 40 random seeds on each task. Figure 1 shows the result of this experiment for three tasks, see Appendix A for the two other tasks. We show both individual runs as well as mean and standard deviations. The variance is often dominated by *outlier runs* that fail to learn early in the training and never recover. E.g. for the walker task, we see several runs which have not improved during the first 500 episodes, and most of these do not improve in the following 500 episodes either. Except for these outliers, the variance of the walker task is relatively small. We also note that these outliers separate themselves relatively early on, suggesting that the issue that causes high variance arises early in training. If it was possible to eliminate poor outlier runs, we would expect the variance to go down. In the following sections, we will investigate different hypotheses for what might cause these bad runs to fail early.

### 3.3 DOES INITIALIZATION MATTER?

There are multiple sources of randomness specific to the early training iterations. The agent networks are randomly initialized and the agent is given some initial experience, collected by random actions, to start training on. Could these two initial factors be the cause of the high variance? To study this hypothesis we measure the correlation between two runs that share the same network initialization and initial experience, but otherwise have independent randomness (from e.g. the environment, action sampling, and mini-batch sampling). Across all tasks, we repeat this process for ten combinations of initializations and initial experience, from each such combination we start two runs  $A, B$  which do not share other sources of randomness. For each time-step  $t$  we measure the Pearson correlation between  $score(A)$  and  $score(B)$ . This correlation, averaged across all timesteps, is shown in Figure 2 (left). We see that the correlation is very small, suggesting that the initialization and initial experience does not have a large effect on the outcome. Specifically, the hypothesis that there are good and bad initializations that leads to good or bad performance is inconsistent with the results of Figure 2 (left). Correlation across time is noisy but centers around zero, see Appendix A.

### 3.4 ARE THE ENVIRONMENTS TOO SENSITIVE?

Another cause of variance is the environments. Perhaps the environments require very specific policies to yield good rewards, and unless the agent stumbles upon a good policy early on, learning fails. To study the sensitivity of the environments we consider gradually exchanging a learned

Table 1: Performance when using contrastive learning or warm starting the convolutional encoder with good weights. Average reward sometimes improves but variance remain high. This suggests that poor features might not cause the high variance. Indeed, Table 2 shows that performance can be improved without better representation learning. Metrics are calculated over 10 seeds.

metric	method	acrobot	finger turn	hopper hop	reacher hard	walker walk
$\mu$	baseline	122.0	278.6	176.2	678.0	769.1
$\mu$	contrastive 10k	141.4	456.2	176.5	671.6	677.1
$\mu$	contrastive 20k	159.4	325.3	209.5	659.6	773.8
$\mu$	warm start	160.0	303.7	153.3	620.8	581.4
$\sigma$	baseline	76.0	221.2	90.3	167.3	350.1
$\sigma$	contrastive 10k	68.4	276.1	104.6	222.4	425.9
$\sigma$	contrastive 20k	67.7	191.9	71.6	164.8	374.4
$\sigma$	warm start	39.8	146.7	86.8	168.7	429.1

policy with a random policy. Specifically, at every timestep  $t$ , with probability  $p$ , we exchange the policy’s action with a random action. The effect of this, for ten final policies learned for the walker environment, is shown in Figure 2 (right). We see that performance degrades gracefully as we gradually move to a random policy. This suggests that the environment is relatively stable with regard to actions. Results for other environments are similar and are shown in Appendix A. Furthermore, in Appendix B we investigate how much variance comes from evaluating the agent on a finite number of episodes. When using ten seeds and ten episodes (the lowest numbers we use), the evaluation variance is dominated by the variance of the random training process. Thus, environment sensitivity and evaluation methodology do not appear to explain the excessive variance.

### 3.5 IS FEATURE LEARNING TO BLAME?

In the early stages of training, the image encoder will extract poor features. Without good representations, it is hard to learn a good policy, and without a policy generating interesting behavior it is hard to learn good representations. If such a vicious cycle was causing runs to fail, jump-starting the encoder to extract good features should help to decrease the variance. To test this hypothesis, we consider initializing the weights of the convolutional encoder to some “good” values. Specifically, for each task, we pick a run with above-average final performance and extract the convolutional weights at episode 500. The encoder is initialized with these good weights but then trained as normal. We refer to this strategy as warm start. In addition to this fix, we also consider improving the features with contrastive learning methods during early training (Laskin et al., 2020b). We use the loss function proposed in Grill et al. (2020) which has been shown to be useful in smaller batch sizes (we use 256) and has already successfully been applied in RL (Schwarzer et al., 2020). We use standard methods in contrastive learning: a target network with exponentially moving weights and a *head* network. See Appendix A for details. We consider adding the contrastive loss to the first 10,000 and 20,000 steps and refer to these modifications as contrastive 10k and contrastive 20k. The results for this experiment are shown in Table 1. For these fixes, the large variance persists even though the performance improves marginally for some environments. We thus hypothesize that representation learning is not the main issue. Indeed, experiments in later sections of the paper show that one can significantly decrease variance without improving representation learning, suggesting that feature quality is not the bottleneck.

## 4 IMPROVING STABILITY

We have considered the effects of initialization, feature learning, and environment sensitivity and found that none of these factors satisfactorily explain the observed variance. Another factor to consider is simply the numerical stability of the learning algorithms. Such learning instability could make the learning process “chaotic”, which would cause high variance. To study this hypothesis we investigate the failure modes of individual runs. In Figure 3 we consider some runs that fail as well as some successful runs for the walker task (which we will use as a running example). Specifically, we plot four quantities during training: rewards, actor gradient norm  $\|\nabla \ell\|$ , actor weight norm  $\|w\|$ ,

and average absolute value of actions  $|a|$ . All agents initially have poor rewards, but once learning starts, the performance improves relatively steadily. During this initial period of no or little learning, the gradients of the actor-network (row two in Figure 3) are small. Similarly, the weight norm of the actor seems to be constant (row three in Figure 3). This suggests that the actor isn't changing its weight much (technically the weights could be "rotating", but this seems unlikely). Why would the actor weights not change? Recall that the actor is optimized by taking gradients:

$$\nabla_{\theta} Q_{\phi}(s, a_{\theta}(s)) = \sum_i \frac{\partial Q_{\phi}}{\partial a_i} \frac{\partial a_i}{\partial \theta} \quad (4)$$

If this gradient is close to zero, we might suspect that  $\frac{\partial a_i}{\partial \theta} \approx 0$ . This could easily happen if the  $\tanh$  non-linearity in equation 3 is saturated. In row four of Figure 3 we show the average absolute value of the actions, which are all bound to lie in  $[-1, 1]$ . We see that for the runs that fail the average absolute action stays around 1 throughout training, which implies that the gradients for the actor are small since  $|\tanh(x)| \approx 1$  implies  $\frac{\partial}{\partial x} \tanh(x) \approx 0$ . The cause of saturating  $\tanh$  must be exploding activations, i.e.  $a_{\theta}^{pre}(s)$  in equation 2 becoming too large, which saturates the  $\tanh$  non-linearity. Exploding activations is a known issue in deep learning (Bjorck et al., 2018; Glorot & Bengio, 2010). In fact, all runs seem to initially suffer from saturating  $\tanh$ , but most runs escape from this poor policy. The Q-values could of course also suffer from instability from exploding activations, although for the walker task the issue seems to mostly come from the policy. These experiments suggest that improving numerical stability and avoiding exploding activations could eliminate failing runs, which in turn would decrease the variance.

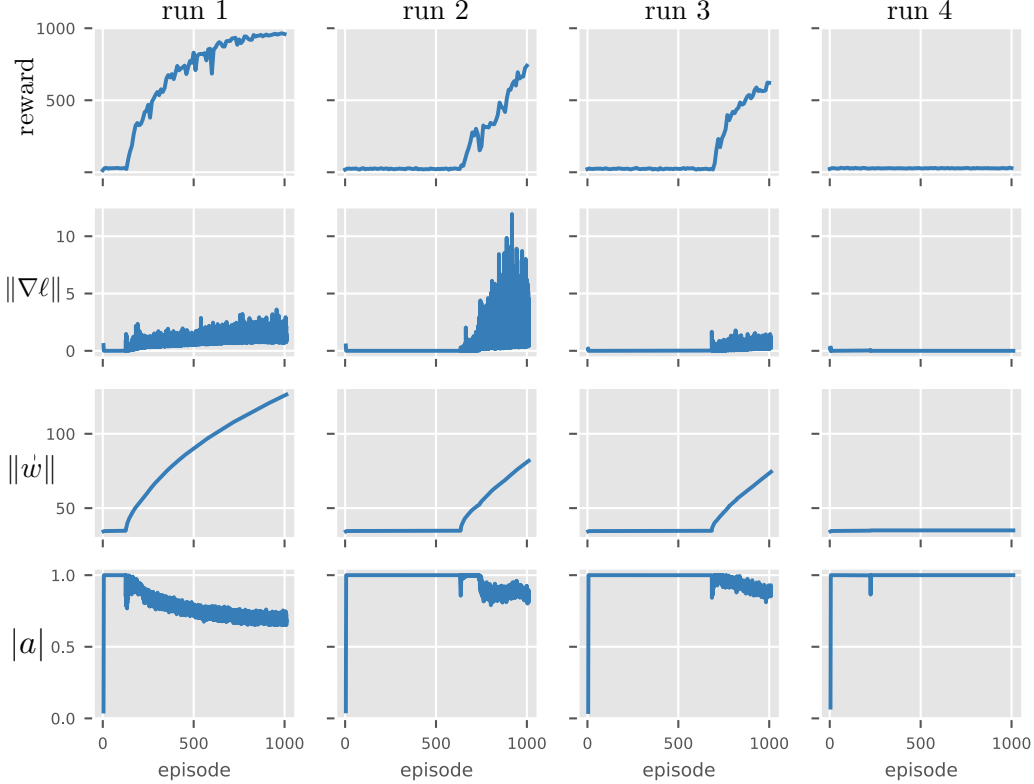


Figure 3: Each row shows a different quantity during training for the baseline agent. Row 1 shows rewards, row 2 shows actor gradient norm  $\|\nabla \ell\|$ , row 3 shows actor weight norm  $\|w\|$  and row 4 shows average absolute action  $|a|$ . Each column corresponds to an independent run of the walker task: run 1 is successful, runs 2 and 3 eventually learn, while run 4 fails to learn. Before learning starts, all runs suffer from small gradients and weights which barely change. During this period, the average absolute value of actions is close to 1. This causes small gradients since the gradient of  $\tanh(x)$  is small when  $|\tanh(x)| \approx 1$ . This suggests that numerical issues may hamper learning.

#### 4.1 TESTING STABILIZATION METHODS

We now consider a few ideas for improving the numerical stability and addressing exploding activations, hoping that these will decrease the variance. We consider four methods:

**Normalizing activations.** Recall that the actor selects actions from the state using  $\mu_\theta(s)$ , where  $\mu_\theta(s)$  is a deep neural network. Figure 3 shows that learning can fail due to exploding activations. To avoid this we propose to parametrize  $\mu_\theta(s)$  as a linear function of features with a fixed magnitude. Specifically, let  $\Lambda_\theta(s)$  be the penultimate features of the actor-network. We propose to simply normalize  $\Lambda_\theta^n(s) = \Lambda_\theta(s)/\|\Lambda_\theta(s)\|$  and let  $\mu$  be a linear function of  $\Lambda_\theta^n$ , i.e.  $\mu_\theta(s) = L\Lambda_\theta^n(s)$  for a linear function  $L$ . We refer to this straightforward modification as *actor norm*. Our motivation has been to stabilize the actor, but the critic might similarly benefit from normalizing penultimate features. We refer to the strategy of normalizing both the actor and the critic as *actor+critic norm*. We also consider *layer norm* (Ba et al., 2016) applied similarly to both the actor and critic.

**Penalizing saturating actions.** Another strategy for avoiding actions with large magnitude is to add a term to the loss function which directly penalizes large actions. One can imagine many such loss functions, we here consider the simple and natural choice of squared loss:

$$\ell(\theta, s) = \lambda \|\mathbf{a}_\theta^{pre}(s)\|^2 \quad (5)$$

We can simply add this to the loss function times some hyperparameter  $\lambda$  and then train the network as normal. By tuning  $\lambda$ , one should be able to remove the saturating actions illustrated in Figure 3. We heuristically find that  $\lambda = 0.000001$  works well in practice (see Appendix A) and use this value. We refer to this modification as *penalty*.

**Learning rate warmup.** One common strategy to improve stability is to start the learning rate at zero and increase it linearly to its top value during early training (Goyal et al., 2017). This can improve numerical stability (Ma & Yarats, 2019). We consider using this strategy and linearly increase the learning rate from zero over the first 10,000 steps. We refer to this strategy as *lr warmup*.

**Gradient clipping.** Another stabilizing strategy is gradient clipping (Zhang et al., 2019). To avoid occasional exploding gradients, one simply clips the norm of gradients that are above some threshold. This strategy is popular in NLP (Gehring et al., 2017; Peters et al., 2018) and is sometimes used in RL (Raffin et al., 2019). We consider clipping the gradient when the norm, calculated independently for the actor, critic, and convolutional encoder, is larger than 1 or 10. We refer to these strategies as *grad clip 1* and *grad clip 10*.

Table 2: Performance for various stability improvements. These methods generally decrease variance, especially for the walker task where variance decreases by orders of magnitude. Larger stability often leads to higher reward, likely as poor outlier runs are eliminated. Normalizing features gives consistent improvements. Metrics are calculated over 10 seeds.

metric	method	acrobot	finger turn	hopper hop	reacher hard	walker walk
$\mu$	baseline	122.0	278.6	176.2	678.0	769.1
$\mu$	penalty	128.0	431.6	241.7	584.6	956.3
$\mu$	actor norm	117.8	372.7	240.5	701.7	956.7
$\mu$	actor+critic norm	192.2	605.8	188.7	892.7	961.5
$\mu$	layer norm	43.5	661.2	218.6	659.7	952.4
$\mu$	lr-warmup	150.3	265.4	173.7	660.9	670.4
$\mu$	grad clip 1	138.2	214.0	206.0	520.0	675.6
$\mu$	grad clip 10	79.3	166.2	157.7	548.4	678.7
$\sigma$	baseline	76.0	221.2	90.3	167.3	350.1
$\sigma$	penalty	42.1	160.6	46.5	236.8	15.4
$\sigma$	actor norm	39.9	227.9	42.7	101.9	8.0
$\sigma$	actor+critic norm	60.1	193.4	78.4	122.5	7.0
$\sigma$	layer norm	57.2	228.4	112.5	297.1	13.5
$\sigma$	lr warmup	53.8	133.6	98.2	133.4	423.4
$\sigma$	grad clip 1	60.6	127.1	92.4	231.9	425.3
$\sigma$	grad clip 10	56.1	143.9	113.6	243.2	426.3

Table 3: Performance when combining three improvements: penultimate feature normalization, action penalty and early contrastive learning. The variance decreases and the performance improves across all tasks. This demonstrates that one can substantially improve variance in RL experiments by simply improving numerical stability. Metrics are calculated over 40 seeds.

metric	method	acrobot	finger turn	hopper hop	reacher hard	walker walk
$\mu$	baseline	122.0	278.6	176.2	678.0	769.1
$\mu$	combined	<b>227.7</b>	<b>653.5</b>	<b>231.1</b>	<b>893.4</b>	<b>964.2</b>
$\sigma$	baseline	76.0	221.2	90.3	167.3	350.1
$\sigma$	combined	<b>59.0</b>	<b>183.1</b>	<b>40.8</b>	<b>120.0</b>	<b>6.2</b>

**Results.** In Table 2 we evaluate the effects of these ideas. We see that it is possible to significantly decrease the variance of the baseline by applying these stabilization methods. Additionally, decreasing the variance increases the average reward – likely as bad outlier runs are eliminated. However, what methods are suitable for what environment varies. The penalty method has relatively mixed performance. Normalizing activations seems to stably improve performance and decrease rewards, whereas layer norm can make performance worse. The performance improvement coming from normalizing the critic suggests that the critic network also suffers from instabilities. Gradient clipping and learning rate warmup perform poorly in comparison. We conclude that feature normalization seems to be the most performant fix, and note that it requires no hyperparameters.

#### 4.2 COMBINING FIXES

We have found that many of the proposed methods can decrease variance and improve average reward. We now consider combining several methods – actor and critic penultimate normalization, pre-tanh penalty, and contrastive learning for the first 10,000 steps – to achieve the best possible performance. In Table 3 we compare the performance between the baseline and an agent using these three modifications (which we refer to as *combined*) over 40 seeds. We see clearly that the variances go down while the average score goes up. In fact, for the walker task, the variance decreases by orders of magnitude. Additionally, eliminating poor outlier runs benefits the average performance in addition to decreasing variance. While our methods have mostly been designed to help outlier runs that fail catastrophically, they likely help more normal runs too. Learning curves for the combined agent are given in Appendix A. Our experiment demonstrates that the perceived variance in RL is not necessarily inherent to the problem definition and may be addressed with minor modifications.

#### 4.3 LEARNING RATE STABILITY

To verify that our fixes indeed increase the stability of learning we now consider changing the learning rate. A high learning rate can cause divergence (Li et al., 2019), and can thus serve as a proxy for learning stability. We consider learning rates in the set  $\{1e-4, 3e-4, 1e-3, 3e-3\}$ , where  $1e-4$  is the default learning rate used by Yarats et al. (2021b). Results for the walker task are shown in Table 4. We see that the baseline algorithm fails for large learning rates, the average rewards drop quickly while variance decreases when no effective policy is learned. With our modifications, the agent can tolerate much higher learning rates while retaining good average rewards and small standard deviation. Learning rate is an important hyperparameter, and it might be possible to further

Table 4: Performance when changing learning rates. The baseline algorithm fails with larger learning rates whereas our combined agent succeeds. This suggests that our fixes improve the stability. Metrics are calculated over 10 seeds on the walker task.

metric	method	1e-4	3e-4	1e-3	3e-3
$\mu$	baseline	769.1	330.2	26.8	25.5
$\mu$	combined	964.2	962.2	954.9	960.1
$\sigma$	baseline	350.1	415.3	3.9	6.4
$\sigma$	combined	6.2	4.7	5.6	5.1



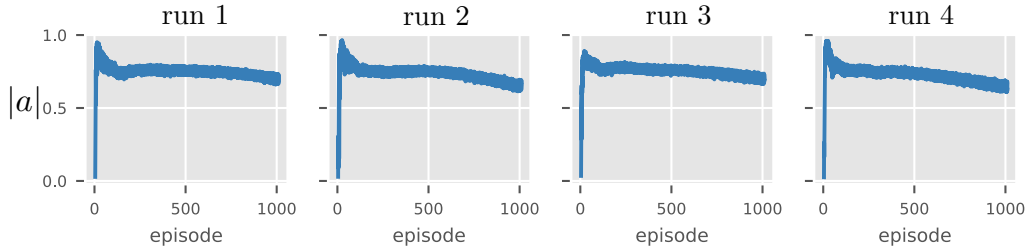


Figure 4: The average absolute value of the actions for the combined agent. We show four representative runs of walker task. Compared to the baseline algorithm (Figure 3), the actions do not saturate early in training despite increasing rapidly. This suggests that our methods improve stability.

improve performance by re-tuning this parameter after our fixes are added. Finally, to verify that the actions do not saturate when using our fixes, we repeat the experiments of Figure 3 with our combined agent. The actions are shown in Figure 4, where we see that the action magnitude indeed goes up quickly early in training but never saturates. This supports our hypothesis that normalizing activations can stabilize training. Further quantities are plotted in Appendix A.

## 5 RELATED WORK

**Variance in RL.** RL is by now commonly accepted to suffer from high variance (Clary et al., 2019; Lynnerup et al., 2020; Henderson et al., 2017; Engstrom et al., 2020). Given this high variance, there is ample work on how to accurately measure performance in RL (Colas et al., 2019). Chan et al. (2019) proposes several metrics that can measure different notations of reliability in reinforcement learning. Jordan et al. (2020) proposes an evaluation methodology that takes into account the effects of hyperparameter tuning. Recently Agarwal et al. (2021) proposes interval estimates of performance. Given this plethora of proposed metrics, we simply report average mean and standard deviation which is commonly reported in practice. Our strategy of simply reducing variance in RL algorithms is complementary to developing robust metrics. Beyond RL, there is work on variance in computer vision Bouthillier et al. (2019) and NLP (Melis et al., 2017; Lin et al., 2021).

**Stabilizing RL.** Within Q-learning, it is known that high variance Q-estimates can impede learning (Fujimoto et al., 2018). Hence, there is a large amount of work on improving the Q-estimates for DQN: averaging weights (Nikishin et al., 2018), averaging Q-estimators (Anschel et al., 2017), using classical variance reduction methods (Jia et al., 2020) and regretted reward (Chen et al., 2018). These papers focus on Q-value variance instead of performance variance and apply to the discrete DQN setting, distinct from continuous control. In policy learning there are several methods for decreasing variance of gradient estimates (Greensmith et al., 2004; Wang et al., 2017), however, these do not directly apply to DDPG. On the architectural side, Parisotto et al. (2020) stabilizes transformers for RL. On the task-specific side, Kumar et al. (2019) stabilizes learning for offline tasks while Mao et al. (2018) considers reducing gradient variance for externally driven environments.

## 6 DISCUSSION

**Limitations.** We have considered a single algorithm on a single suite of tasks. Our setting uses a state-of-the-art method on a popular benchmark relatively close to real-world applications. Nonetheless, many important settings remain, e.g. model-based algorithms (Hafner et al., 2020) and discrete environments (Bellemare et al., 2013). This paper shows that *it is possible* to decrease variance with simple modifications, although which methods are effective likely depends upon the base algorithm. We leave evaluating how well our modifications transfer to other settings for future work.

**Conclusion.** We have investigated causes of variance in a popular continuous control setup. Whereas feature learning and network initialization do not appear to be at fault, we observe that learning instability causes significant variance. We show that simply normalizing the features has a stabilizing effect that decreases the variance and also propose several additional fixes. Our experiments demonstrate that the perception that RL has intrinsically high variance might need to be revisited – in some cases, numerical issues might instead be at fault.

---

**Ethics Statement.** There are many positive RL applications – examples include safe autonomous cars, accelerated scientific discovery, and medical testing. Studying causes of high variance, and proposing fixes to this issue, can benefit real-world adoption of RL techniques. Additionally, reducing the variance of RL experiments would aid the research community as reproducibility can be problematic in the field. However, there are also many potentially harmful military applications. Our study is academic in nature and only considers simulated toy environments, but insights from our work could nonetheless be useful in harmful applications. We do not believe that our work differs from other RL work significantly with regard to ethics.

**Reproducibility Statement.** In Appendix A we detail the infrastructure and software used. The perhaps most important component of generating reproducible findings in RL is to use many seeds. To this end, we only consider five environments but evaluated these thoroughly. The main experiments of the paper (Table 3) use 40 seeds whereas all others use 10 seeds.

**Acknowledgement.** This research is supported in part by the grants from the National Science Foundation (III-1618134, III-1526012, IIS1149882, IIS-1724282, and TRIPODS- 1740822), the Office of Naval Research DOD (N00014- 17-1-2175), Bill and Melinda Gates Foundation. We are thankful for generous support by Zillow and SAP America Inc. This material is based upon work supported by the National Science Foundation under Grant Number CCF-1522054. We are also grateful for support through grant AFOSR-MURI (FA9550-18-1-0136). Any opinions, findings, conclusions, or recommendations expressed here are those of the authors and do not necessarily reflect the views of the sponsors. We thank Rich Bernstein, Wenting Zhao and Ziwei Liu for help with the manuscript.

## REFERENCES

- Rishabh Agarwal, Max Schwarzer, Pablo Samuel Castro, Aaron Courville, and Marc G Bellemare. Deep reinforcement learning at the edge of the statistical precipice. *arXiv preprint arXiv:2108.13264*, 2021.
- Oron Anschel, Nir Baram, and Nahum Shimkin. Averaged-dqn: Variance reduction and stabilization for deep reinforcement learning. In *International conference on machine learning*, pp. 176–185. PMLR, 2017.
- Jimmy Lei Ba, Jamie Ryan Kiros, and Geoffrey E Hinton. Layer normalization. *arXiv preprint arXiv:1607.06450*, 2016.
- Philip Bachman, R Devon Hjelm, and William Buchwalter. Learning representations by maximizing mutual information across views. *arXiv preprint arXiv:1906.00910*, 2019.
- Hamsa Bastani, Kimon Drakopoulos, Vishal Gupta, Jon Vlachogiannis, Christos Hadjicristodoulou, Pagona Lagiou, Gkikas Magiorkinis, Dimitrios Paraskevis, and Sotirios Tsiodras. Efficient and targeted covid-19 border testing via reinforcement learning, 2021.
- Marc G Bellemare, Yavar Naddaf, Joel Veness, and Michael Bowling. The arcade learning environment: An evaluation platform for general agents. *Journal of Artificial Intelligence Research*, 47: 253–279, 2013.
- Marc G Bellemare, Salvatore Candido, Pablo Samuel Castro, Jun Gong, Marlos C Machado, Subhdeep Moitra, Sameera S Ponda, and Ziyu Wang. Autonomous navigation of stratospheric balloons using reinforcement learning. *Nature*, 588(7836):77–82, 2020.
- Johan Bjorck, Carla Gomes, Bart Selman, and Kilian Q Weinberger. Understanding batch normalization. *arXiv preprint arXiv:1806.02375*, 2018.
- Xavier Bouthillier, César Laurent, and Pascal Vincent. Unreproducible research is reproducible. In *International Conference on Machine Learning*, pp. 725–734. PMLR, 2019.
- Xavier Bouthillier, Pierre Delaunay, Mirko Bronzi, Assya Trofimov, Brennan Nichyporuk, Justin Szeto, Nazanin Mohammadi Sepahvand, Edward Raff, Kanika Madan, Vikram Voleti, et al. Accounting for variance in machine learning benchmarks. *Proceedings of Machine Learning and Systems*, 3, 2021.

- 
- Stephanie CY Chan, Samuel Fishman, John Canny, Anoop Korattikara, and Sergio Guadarrama. Measuring the reliability of reinforcement learning algorithms. *arXiv preprint arXiv:1912.05663*, 2019.
- Shi-Yong Chen, Yang Yu, Qing Da, Jun Tan, Hai-Kuan Huang, and Hai-Hong Tang. Stabilizing reinforcement learning in dynamic environment with application to online recommendation. In *Proceedings of the 24th ACM SIGKDD International Conference on Knowledge Discovery & Data Mining*, pp. 1187–1196, 2018.
- Ting Chen, Simon Kornblith, Mohammad Norouzi, and Geoffrey Hinton. A simple framework for contrastive learning of visual representations. In *International conference on machine learning*, pp. 1597–1607. PMLR, 2020.
- Kaleigh Clary, Emma Tosch, John Foley, and David Jensen. Let’s play again: Variability of deep reinforcement learning agents in atari environments. *arXiv preprint arXiv:1904.06312*, 2019.
- Cédric Colas, Olivier Sigaud, and Pierre-Yves Oudeyer. How many random seeds? statistical power analysis in deep reinforcement learning experiments. *arXiv preprint arXiv:1806.08295*, 2018.
- Cédric Colas, Olivier Sigaud, and Pierre-Yves Oudeyer. A hitchhiker’s guide to statistical comparisons of reinforcement learning algorithms. *arXiv preprint arXiv:1904.06979*, 2019.
- Logan Engstrom, Andrew Ilyas, Shibani Santurkar, Dimitris Tsipras, Firdaus Janoos, Larry Rudolph, and Aleksander Madry. Implementation matters in deep policy gradients: A case study on ppo and trpo. *arXiv preprint arXiv:2005.12729*, 2020.
- Scott Fujimoto, Herke Hoof, and David Meger. Addressing function approximation error in actor-critic methods. In *International Conference on Machine Learning*, pp. 1587–1596. PMLR, 2018.
- Javier Garcia and Fernando Fernández. A comprehensive survey on safe reinforcement learning. *Journal of Machine Learning Research*, 16(1):1437–1480, 2015.
- Jonas Gehring, Michael Auli, David Grangier, Denis Yarats, and Yann N Dauphin. Convolutional sequence to sequence learning. In *International Conference on Machine Learning*, pp. 1243–1252. PMLR, 2017.
- Xavier Glorot and Yoshua Bengio. Understanding the difficulty of training deep feedforward neural networks. In *Proceedings of the thirteenth international conference on artificial intelligence and statistics*, pp. 249–256. JMLR Workshop and Conference Proceedings, 2010.
- Priya Goyal, Piotr Dollár, Ross Girshick, Pieter Noordhuis, Lukasz Wesolowski, Aapo Kyrola, Andrew Tulloch, Yangqing Jia, and Kaiming He. Accurate, large minibatch sgd: Training imagenet in 1 hour. *arXiv preprint arXiv:1706.02677*, 2017.
- Evan Greensmith, Peter L Bartlett, and Jonathan Baxter. Variance reduction techniques for gradient estimates in reinforcement learning. *Journal of Machine Learning Research*, 5(9), 2004.
- Jean-Bastien Grill, Florian Strub, Florent Altché, Corentin Tallec, Pierre H Richemond, Elena Buchatskaya, Carl Doersch, Bernardo Avila Pires, Zhaohan Daniel Guo, Mohammad Gheshlaghi Azar, et al. Bootstrap your own latent: A new approach to self-supervised learning. *arXiv preprint arXiv:2006.07733*, 2020.
- Tuomas Haarnoja, Aurick Zhou, Pieter Abbeel, and Sergey Levine. Soft actor-critic: Off-policy maximum entropy deep reinforcement learning with a stochastic actor. *arXiv preprint arXiv:1801.01290*, 2018.
- Danijar Hafner, Timothy Lillicrap, Mohammad Norouzi, and Jimmy Ba. Mastering atari with discrete world models. *arXiv preprint arXiv:2010.02193*, 2020.
- Kaiming He, Haoqi Fan, Yuxin Wu, Saining Xie, and Ross Girshick. Momentum contrast for unsupervised visual representation learning. *arXiv preprint arXiv:1911.05722*, 2019.
- Peter Henderson, Riashat Islam, Philip Bachman, Joelle Pineau, Doina Precup, and David Meger. Deep reinforcement learning that matters. *arXiv preprint arXiv:1709.06560*, 2017.

- 
- Haonan Jia, Xiao Zhang, Jun Xu, Wei Zeng, Hao Jiang, Xiaohui Yan, and Ji-Rong Wen. Variance reduction for deep q-learning using stochastic recursive gradient. *arXiv preprint arXiv:2007.12817*, 2020.
- Scott Jordan, Yash Chandak, Daniel Cohen, Mengxue Zhang, and Philip Thomas. Evaluating the performance of reinforcement learning algorithms. In *International Conference on Machine Learning*, pp. 4962–4973. PMLR, 2020.
- B Ravi Kiran, Ibrahim Sobh, Victor Talpaert, Patrick Mannion, Ahmad A Al Sallab, Senthil Yogamani, and Patrick Pérez. Deep reinforcement learning for autonomous driving: A survey. *IEEE Transactions on Intelligent Transportation Systems*, 2021.
- Ilya Kostrikov, Denis Yarats, and Rob Fergus. Image augmentation is all you need: Regularizing deep reinforcement learning from pixels. 2020.
- Aviral Kumar, Justin Fu, George Tucker, and Sergey Levine. Stabilizing off-policy q-learning via bootstrapping error reduction. *arXiv preprint arXiv:1906.00949*, 2019.
- Michael Laskin, Kimin Lee, Adam Stooke, Lerrel Pinto, Pieter Abbeel, and Aravind Srinivas. Reinforcement learning with augmented data. *arXiv preprint arXiv:2004.14990*, 2020a.
- Michael Laskin, Aravind Srinivas, and Pieter Abbeel. Curl: Contrastive unsupervised representations for reinforcement learning. In *Proceedings of the 37th Annual International Conference on Machine Learning (ICML)*, 2020b.
- Yuanzhi Li, Colin Wei, and Tengyu Ma. Towards explaining the regularization effect of initial large learning rate in training neural networks. *arXiv preprint arXiv:1907.04595*, 2019.
- Timothy P Lillicrap, Jonathan J Hunt, Alexander Pritzel, Nicolas Heess, Tom Erez, Yuval Tassa, David Silver, and Daan Wierstra. Continuous control with deep reinforcement learning. *arXiv preprint arXiv:1509.02971*, 2015.
- Jimmy Lin, Daniel Campos, Nick Craswell, Bhaskar Mitra, and Emine Yilmaz. Significant improvements over the state of the art? a case study of the ms marco document ranking leaderboard. *arXiv preprint arXiv:2102.12887*, 2021.
- Yan Liu, Zhiyuan Jiang, Shunqing Zhang, and Shugong Xu. Deep reinforcement learning-based beam tracking for low-latency services in vehicular networks. In *ICC 2020-2020 IEEE International Conference on Communications (ICC)*, pp. 1–7. IEEE, 2020.
- Nicolai A Lynnerup, Laura Nolling, Rasmus Hasle, and John Hallam. A survey on reproducibility by evaluating deep reinforcement learning algorithms on real-world robots. In *Conference on Robot Learning*, pp. 466–489. PMLR, 2020.
- Jerry Ma and Denis Yarats. On the adequacy of untuned warmup for adaptive optimization. *arXiv preprint arXiv:1910.04209*, 7, 2019.
- Hongzi Mao, Shaileshh Bojja Venkatakrishnan, Malte Schwarzkopf, and Mohammad Alizadeh. Variance reduction for reinforcement learning in input-driven environments. *arXiv preprint arXiv:1807.02264*, 2018.
- Gábor Melis, Chris Dyer, and Phil Blunsom. On the state of the art of evaluation in neural language models. *arXiv preprint arXiv:1707.05589*, 2017.
- Volodymyr Mnih, Koray Kavukcuoglu, David Silver, Andrei A Rusu, Joel Veness, Marc G Belle-mare, Alex Graves, Martin Riedmiller, Andreas K Fidjeland, Georg Ostrovski, et al. Human-level control through deep reinforcement learning. *nature*, 518(7540):529–533, 2015.
- Evgenii Nikishin, Pavel Izmailov, Ben Athiwaratkun, Dmitrii Podoprikin, Timur Garipov, Pavel Shvechikov, Dmitry Vetrov, and Andrew Gordon Wilson. Improving stability in deep reinforcement learning with weight averaging. In *Uncertainty in artificial intelligence workshop on uncertainty in Deep learning*, 2018.

- 
- Emilio Parisotto, Francis Song, Jack Rae, Razvan Pascanu, Caglar Gulcehre, Siddhant Jayakumar, Max Jaderberg, Raphael Lopez Kaufman, Aidan Clark, Seb Noury, et al. Stabilizing transformers for reinforcement learning. In *International Conference on Machine Learning*, pp. 7487–7498. PMLR, 2020.
- Matthew E Peters, Mark Neumann, Mohit Iyyer, Matt Gardner, Christopher Clark, Kenton Lee, and Luke Zettlemoyer. Deep contextualized word representations. *arXiv preprint arXiv:1802.05365*, 2018.
- Antonin Raffin, Ashley Hill, Maximilian Ernestus, Adam Gleave, Anssi Kanervisto, and Noah Dornmann. Stable baselines3. <https://github.com/DLR-RM/stable-baselines3>, 2019.
- Max Schwarzer, Ankesh Anand, Rishab Goel, R Devon Hjelm, Aaron Courville, and Philip Bachman. Data-efficient reinforcement learning with momentum predictive representations. *arXiv preprint arXiv:2007.05929*, 2020.
- David Silver, Julian Schrittwieser, Karen Simonyan, Ioannis Antonoglou, Aja Huang, Arthur Guez, Thomas Hubert, Lucas Baker, Matthew Lai, Adrian Bolton, et al. Mastering the game of go without human knowledge. *nature*, 550(7676):354–359, 2017.
- Krishnan Srinivasan, Benjamin Eysenbach, Sehoon Ha, Jie Tan, and Chelsea Finn. Learning to be safe: Deep rl with a safety critic. *arXiv preprint arXiv:2010.14603*, 2020.
- Richard S Sutton. Learning to predict by the methods of temporal differences. *Machine learning*, 3(1):9–44, 1988.
- Richard S Sutton and Andrew G Barto. *Reinforcement learning: An introduction*. MIT press, 2018.
- Yuval Tassa, Saran Tunyasuvunakool, Alistair Muldal, Yotam Doron, Siqi Liu, Steven Bohez, Josh Merel, Tom Erez, Timothy Lillicrap, and Nicolas Heess. dm control: Software and tasks for continuous control, 2020.
- Tongzhou Wang, Yi Wu, David A Moore, and Stuart J Russell. Meta-learning mcmc proposals. *arXiv preprint arXiv:1708.06040*, 2017.
- Christopher John Cornish Hellaby Watkins. Learning from delayed rewards. 1989.
- Denis Yarats, Rob Fergus, Alessandro Lazaric, and Lerrel Pinto. Mastering visual continuous control: Improved data-augmented reinforcement learning. *arXiv preprint arXiv:2107.09645*, 2021a.
- Denis Yarats, Rob Fergus, Alessandro Lazaric, and Lerrel Pinto. Mastering visual continuous control: Improved data-augmented reinforcement learning. *arXiv preprint arXiv:2107.09645*, 2021b.
- Albert Zhan, Philip Zhao, Lerrel Pinto, Pieter Abbeel, and Michael Laskin. A framework for efficient robotic manipulation. *arXiv preprint arXiv:2012.07975*, 2020.
- Jingzhao Zhang, Tianxing He, Suvrit Sra, and Ali Jadbabaie. Why gradient clipping accelerates training: A theoretical justification for adaptivity. *arXiv preprint arXiv:1905.11881*, 2019.
- Henry Zhu, Justin Yu, Abhishek Gupta, Dhruv Shah, Kristian Hartikainen, Avi Singh, Vikash Kumar, and Sergey Levine. The ingredients of real-world robotic reinforcement learning. *arXiv preprint arXiv:2004.12570*, 2020.

## A APPENDIX

**Tuning  $\lambda$ .** For tuning the hyperparameters  $\lambda$  defined in equation 5 we search over the set  $\{1e-1, 1e-2, 1e-3, 1e-4, 1e-5, 1e-6\}$ . For each value, we run the hopper task for a short amount of time with five different seeds. We found that too large  $\lambda$  penalized actions too much, and that even very small values like  $1e-6$  sufficed to give improvement.

**Details on Contrastive Learning.** We extract features from the convolutional network and the first feedforward layer of the critic, which projects the feature map to 50-dimensions. Feature vectors are normalized to unit norm before being fed into the contrastive loss (Bachman et al., 2019). We use exponentially moving weights for the target contrastive network (He et al., 2019), using the same decay parameters as for the target critic. We use a *head* for the online network which is simply a two-layer MLP with hidden dimension 512 and final dimension 50 (Chen et al., 2020). The two augmentations we consider are simply two adjacent frames with augmentations that the DDPG agent of Yarats et al. (2021b) considers naturally. We use the square loss as proposed in Grill et al. (2020), which has been shown to be useful in smaller batch sizes. The contrastive loss is then simply added to the normal loss function for the critic.

**Infrastructure.** We run our experiments on Nvidia Tesla V100 GPUs and Intel Xeon CPUs. The GPUs use CUDA 11.1 and CUDNN 8.0.0.5. We use PyTorch 1.9.0 and python 3.8.10. Our experiments are all based upon the open-source implementation of Yarats et al. (2021b).

Table 5: Variance across tasks as reported by Yarats et al. (2021b). Mean reward and task variance often increase in tandem – to avoid bias towards easy tasks with high mean and thus high variance, we rank tasks based upon relative variance  $\sigma/\mu$ . We use the five tasks with the highest relative variance, removing one duplicate: finger turn easy/hard. Used tasks are highlighted. Scores are measured just before 1 million frames (i.e. frame 980000) since not all runs have scores at the 1 million mark. All numbers are rounded to two decimal digits.

task	$\sigma/\mu$	$\mu$	$\sigma$
finger turn hard	0.74	268.90	198.36
walker walk	0.48	769.66	371.48
hopper hop	0.36	221.13	80.63
finger turn easy	0.31	558.52	174.19
acrobot swingup	0.31	177.65	54.77
reacher hard	0.22	628.29	135.57
walker run	0.20	538.59	110.02
cup catch	0.13	909.95	118.06
finger spin	0.12	860.30	104.18
quadruped run	0.12	446.49	53.51
quadruped walk	0.12	732.52	87.19
cartpole balance sparse	0.12	962.30	113.10
reach duplo	0.08	202.51	16.99
cartpole swingup sparse	0.08	760.11	60.11
cheetah run	0.07	710.24	52.43
reacher easy	0.05	931.54	50.86
pendulum swingup	0.04	838.49	36.38
hopper stand	0.02	917.85	20.45
cartpole swingup	0.02	864.68	15.47
walker stand	0.01	980.72	5.21
cartpole balance	0.01	993.45	5.00

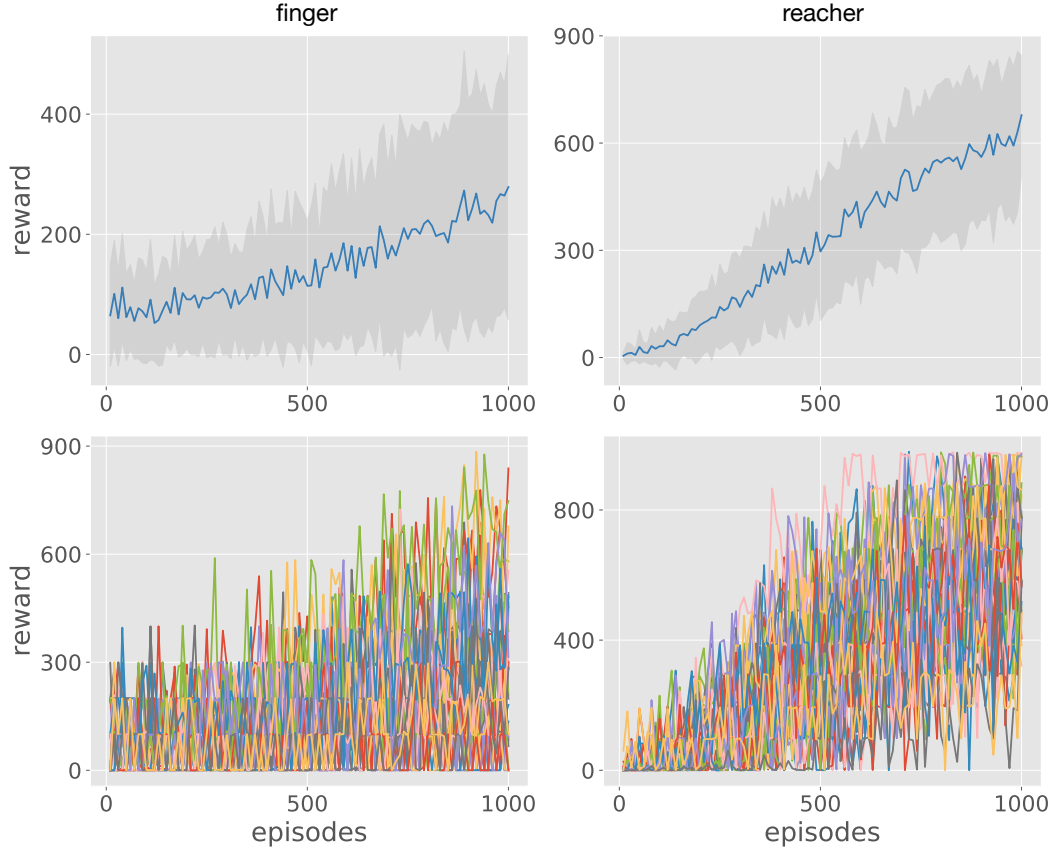


Figure 5: Learning curves for the two tasks not shown in Figure 1. The upper row shows the mean reward with one standard deviation indicated by shading. The bottom row show learning curves for individual runs. Although the signal is noisy, several outlier runs fail to learn.

Table 6: Hyperparameters used throughout the paper. These follow Yarats et al. (2021b) for the *medium* tasks.

parameter	value
learning rate	$1e-4$
soft-update $\tau$	$1e-2$
update frequency	2
stddev. schedule	$\text{linear}(1.0, 0.1, 500000)$
stddev. clip	0.3
action repeat	2
seed frames	$4e3$
batch size	256
$n$ -step returns	3
discount $\gamma$	0.99

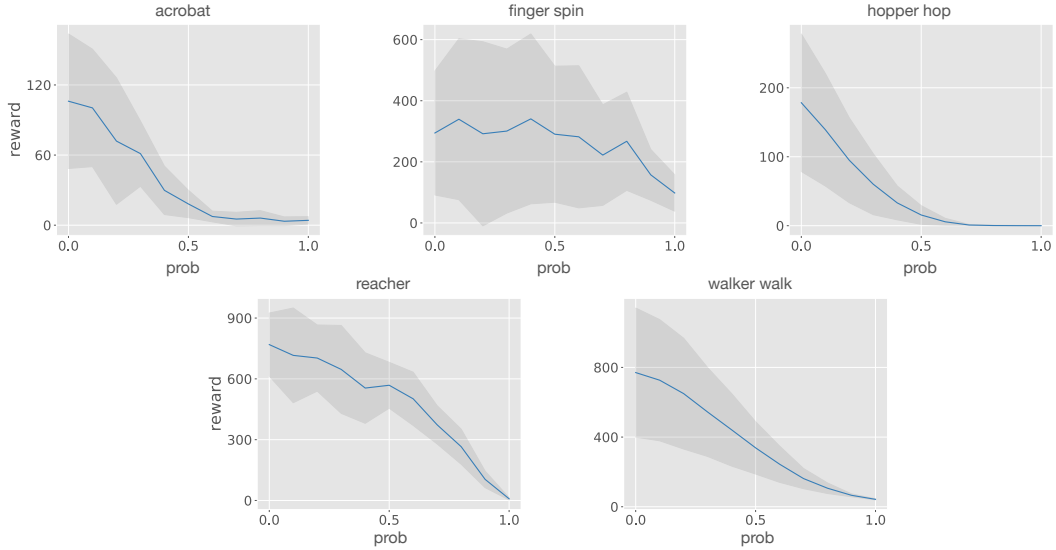


Figure 6: Rewards obtained when gradually replacing a learned policy with a random policy. At every time-step  $t$ , the action suggested by the learned policy is replaced with a random action with probability  $p$ . We start from the final policy learned by the baseline algorithm and average over ten starting policies. Across all tasks, the rewards decrease gracefully with a more random policy, suggesting that the environments are robust to perturbed policies.

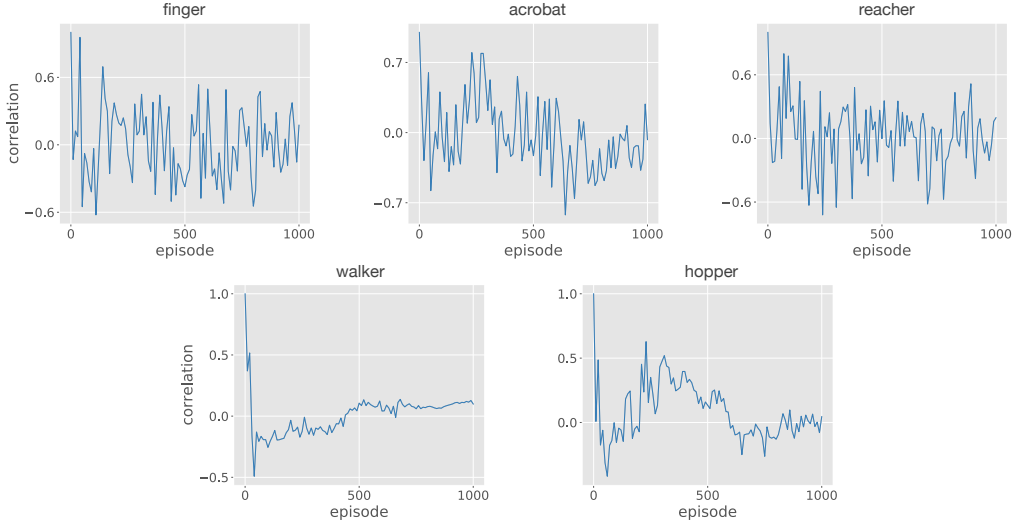


Figure 7: Correlation between the evaluation scores of two runs that share network initialization and seed experience, but otherwise have different randomness. Correlation is calculated across ten runs and plotted against time. The correlation is noisy for many environments but oscillates around zero, suggesting that there is little actual correlation and that network initialization and seed experience have a small effect.



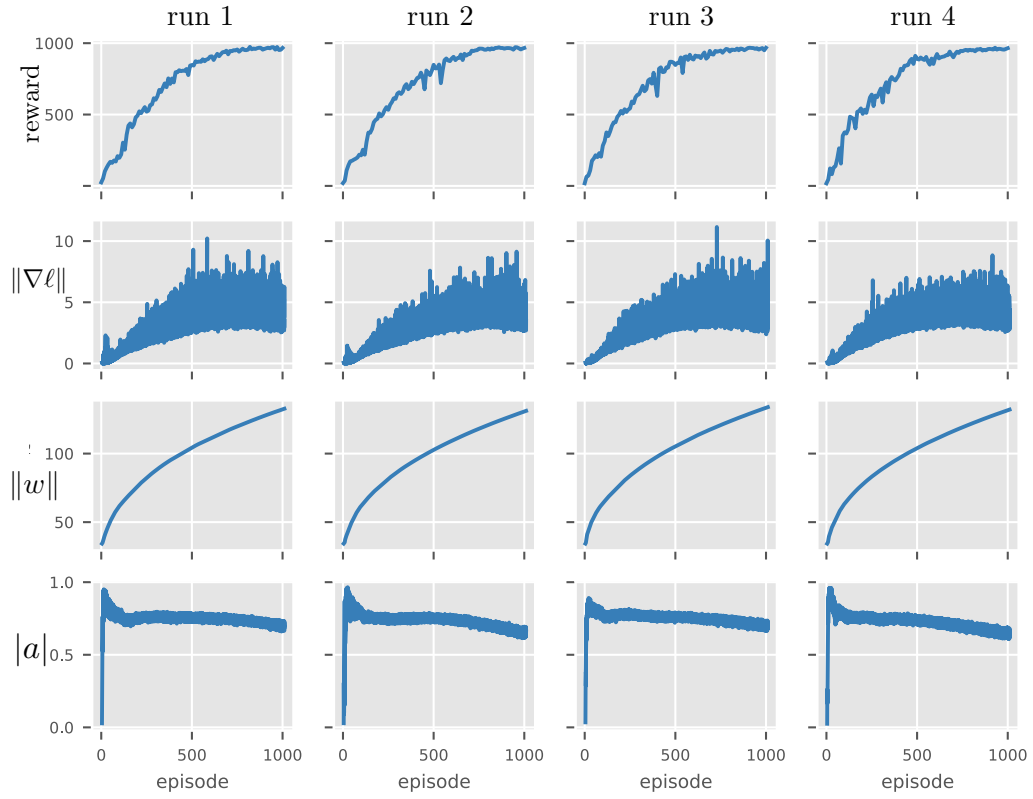


Figure 8: Four quantities shown during training for the combined agent. We show reward, norm of actor gradient  $\|\nabla\ell\|$ , norm of actor weight  $\|w\|$  and average absolute action  $|a|$ . The actions never saturate and learning starts quickly. Compare with Figure 3, which shows the same quantities for the baseline algorithm.

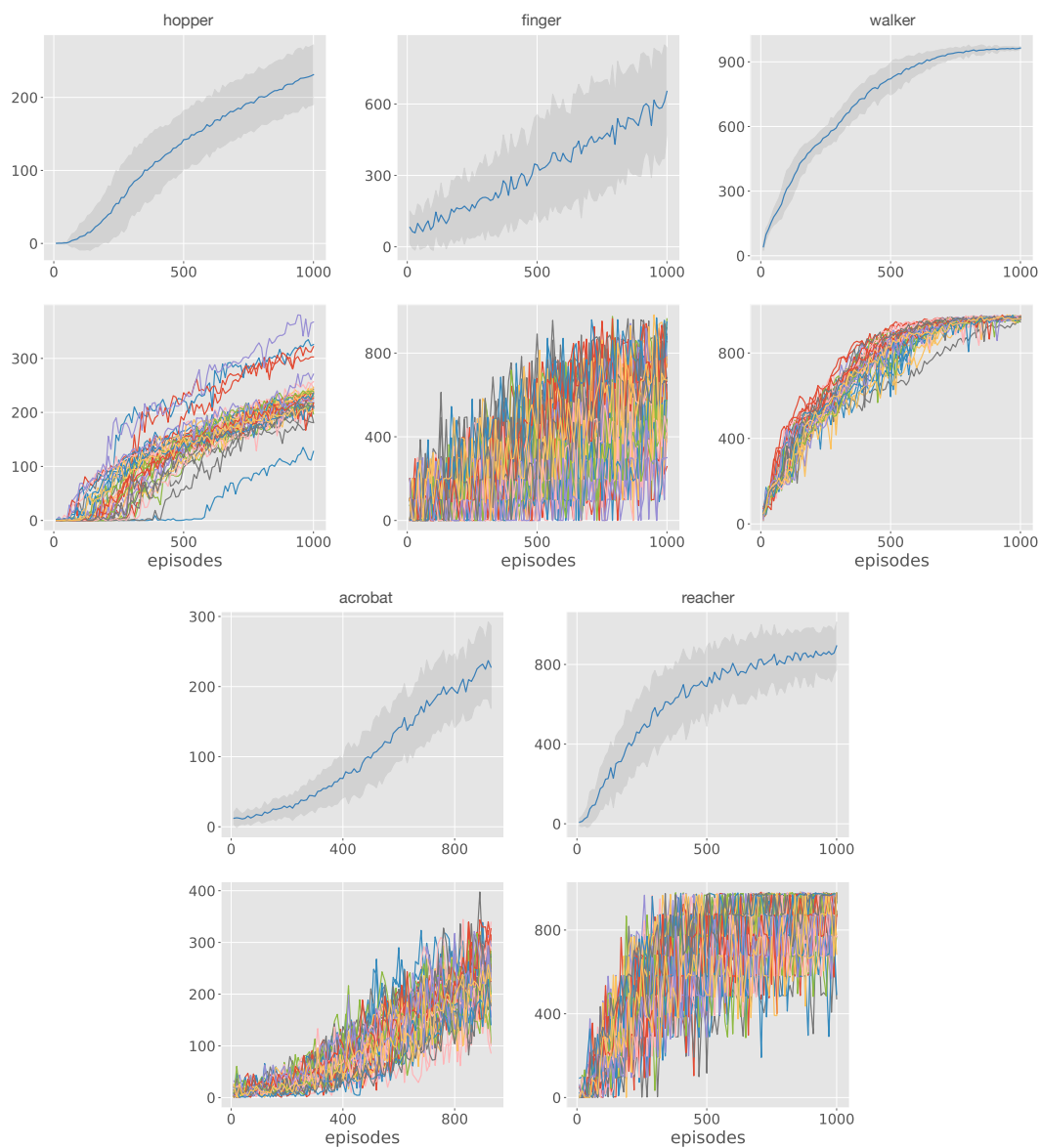


Figure 9: Learning curves when using our combined agent. We show mean reward with one standard deviation indicated by shading and learning curves for individual runs.

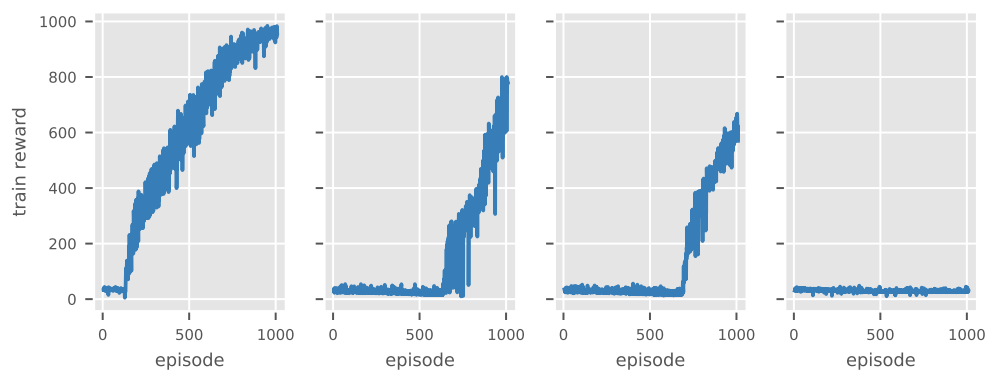


Figure 10: Rewards obtained during training for the runs illustrated in Figure 3. Note that the rewards are nonzero from the start of training. This implies that the agent observes rewards and can train on these. Thus, lack of rewards is not the cause of the poor performance.

## B EVALUATION VARIANCE

We will now consider the variance arising from evaluating RL agents on a finite set of episodes. Similar to the bias-variance decomposition, we will see that the variance here can be divided into one part that depends upon the randomness of the algorithm, and one term that depends on the randomness from the finite set of episodes we evaluate on. We let  $R$  be a set of training runs and  $S$  be a set of evaluation episodes sampled. The performance is measured by

$$\text{perf} = \frac{1}{|R||S|} \sum_{i \in R} \sum_{j \in S} r_{ij}$$

Let us calculate the variance of this quantity. We will assume that rewards from different runs are independent, and that rewards from the same training run are independent conditioned on that run. We now have

$$\text{Var}\left(\frac{1}{|R||S|} \sum_{i \in R} \sum_{j \in S} r_{ij}\right)$$

The variance of a sum of independent variables is simply the sum of their variances. Thus we have

$$\text{Var}\left(\frac{1}{|R||S|} \sum_{i \in R} \sum_{j \in S} r_{ij}\right) = \frac{1}{|R|} \text{Var}\left(\frac{1}{|S|} \sum_{j \in S} r_{ij}\right)$$

Let  $\mu = \mathbb{E}[r_{ij}]$ . We then have

$$\text{Var}\left(\frac{1}{|S|} \sum_{j \in S} r_{ij}\right) = \mathbb{E}_{alg, samples} \left[ \left( \frac{1}{|S|} \sum_{j \in S} r_{ij} - \mu \right)^2 \right]$$

Here we explicitly calculate the expectation over random training runs (*alg*) and the random episodes sampled (*samples*). We can condition the expectation upon the random training run and then integrate over this expectation. Furthermore, let  $\mu_i = \mathbb{E}[r_{ij}|i]$ , i.e. the expected value an episode sampled from training run  $i$ . We then have

$$\begin{aligned} \text{Var}\left(\frac{1}{|S|} \sum_{j \in S} r_{ij}\right) &= \mathbb{E}_{alg} \left[ \mathbb{E}_{samples} \left[ \left( \frac{1}{|S|} \sum_{j \in S} r_{ij} - \mu \right)^2 \middle| i \right] \right] \\ &= \mathbb{E}_{alg} \left[ \mathbb{E}_{samples} \left[ \left( \frac{1}{|S|} \sum_{j \in S} r_{ij} - \mu_i + \mu_i - \mu \right)^2 \middle| i \right] \right] \\ &= \mathbb{E}_{alg} \left[ \mathbb{E}_{samples} \left[ \left( \frac{1}{|S|} \sum_{j \in S} r_{ij} - \mu_i \right)^2 \middle| i \right] \right] \\ &\quad + 2\mathbb{E}_{samples} \left[ \left( \frac{1}{|S|} \sum_{j \in S} r_{ij} - \mu_i \right) (\mu_i - \mu) \middle| i \right] \\ &\quad + \mathbb{E}_{samples} \left[ (\mu_i - \mu)^2 \middle| i \right] \end{aligned}$$

The middle part vanishes since  $\mu_i = \mathbb{E}[r_{ij}|i]$ . For the first term, given a fixed training run the terms  $r_{ij}$  are independent. This gives us

Table 7: Sample variance and algorithm variance as defined in eq. (6). Some tasks have high variance and others have low. However, sampling more episodes does not decrease variance considerable in the 10 training seeds and 10 episodes setting, see eq. (7).

method	walker walk	hopper hop	finger turn	acrobot	reacher reach
sample	1922.1	450.6	143763.0	11182.9	176211.9
alg	80002.6	9774.0	55215.6	5710.9	35231.7

$$\begin{aligned}
\mathbb{E}_{alg} \left[ \mathbb{E}_{samples} \left[ \left( \frac{1}{|S|} \sum_{j \in S} r_{ij} - \mu_i \right)^2 \middle| i \right] \right] &= \frac{1}{|S|^2} \mathbb{E}_{alg} \left[ \mathbb{E}_{samples} \left[ \left( \sum_{j \in S} r_{ij} - |S| \mu_i \right)^2 \middle| i \right] \right] \\
&= \frac{1}{|S|^2} \mathbb{E}_{alg} \left[ \mathbb{E}_{samples} \left[ \sum_{j \in S} (r_{ij} - \mu_i)^2 \middle| i \right] \right] = \frac{1}{|S|} \mathbb{E}_{alg} \left[ \mathbb{E}_{samples} \left[ (r_{ij} - \mu_i)^2 \middle| i \right] \right]
\end{aligned}$$

We then have

$$\text{Var}(\text{perf}) = \frac{1}{|R|} \underbrace{\mathbb{E}_{alg}[(\mu_{alg} - \mu)^2]}_{\text{algorithm variance}} + \frac{1}{|R||S|} \underbrace{\mathbb{E}_{alg}[\mathbb{E}_{samples}[(r - \mu_{alg})^2 | i]]}_{\text{sample variance}} \quad (6)$$

Here  $\mu_{alg} = \mu_i$ . The first term is what we are interested in measuring. The second term can be large if the environment is noisy and we sample too few episodes. The second term is straightforward to estimate: run the algorithm N times and measure the performance over M samples. For each run, calculate the variance over the samples. Then average this variance over all runs.

In Table 7 we estimate these quantities over ten training runs and ten episodes for the baseline algorithm. As we can see, the environments have very different characteristics. Some have high sample variance and some have very low sample variance. It is common to evaluate with ten training seeds and ten episodes. Can we improve the variance by evaluating on more episodes, say 100? Even for the task with the highest sample noise (reacher), the relative improvement in the standard deviation of the sample variance, i.e.,

$$\sqrt{(\sigma_{alg}^2 + \frac{1}{10} \sigma_{sample}^2) / (\sigma_{alg}^2 + \frac{1}{100} \sigma_{sample}^2)} \approx 1.195 \quad (7)$$

is no larger than 20 %. Thus, we conclude that only minor gains can come from evaluating on more episodes. Other environments outside the five we consider, however, might benefit more from using more samples.